HIGHLY EXTENSIBLE WAVY-PLY SANDWICH WITH COMPOSITE SKINS AND CRUSHABLE CORE

S. Pimenta*[1], P. Robinson[2]

[1] *Dept. Mechanical Engineering, Imperial College London, SW7 2AZ London, UK*
[2] *The Composites Centre, Dept Aeronautics, Imperial College London, SW7 2AZ London, UK*
* *Corresponding Author: soraia.pimenta@imperial.ac.uk*

Keywords: Sandwich structures, Finite Elements, Mechanical testing, Large deformations

Abstract

This work proposes a new design for sandwich structures with wavy skins and a crushable core, aiming to achieve large deformations and energy absorption under tensile loading. Optimised geometries, designed by analytical and finite element modelling and manufactured using carbon–epoxy skins and a PMI foam core, exhibited an average failure strain of 8.6%*, a work of fracture of* 9.4 kJ/kg*, and ultimate strength of* 1570 MPa*.*

1. Introduction

Fibre–Reinforced Polymers (FRPs) are remarkably stiff and strong materials, but their restricted ability to deform and withstand damage limits their applicability. This work proposes a sandwich structure with symmetric wavy skins and a crushable core (illustrated in Figure 1), which aims to achieve (i) large deformations (through fibre re-orientation), (ii) energy absorption (through crushing of the core), and (iii) a stable non-linear tensile response (with no significant load drops before final failure).

The wavy–ply sandwich concept is designed for in–plane tensile loading (see Figure 1) and relies on the following three components:

- *Wavy skins*: the skins are the main load–carrying element. Their initial waviness will provide excess length during tensile loading, allowing for large remote extensions through unfolding. The skins will be manufactured with Carbon–Fibre Reinforced–Polymer (CFRP) with tough epoxy matrix (Hexcel M21/35%/198/T800S);
- *Crushable core*: while the core should provide initial stiffness to the system, it will allow the wavy skins to unfold with further loading and absorb energy through crushing. The crushable core cells will be machined from Evonik Rohacell RIMA foam (high–performance closed–cell PMI–based foams, specifically developed for minimal resin absorption), and co-cured with the composite wavy skins;
- *Bridging region*: the bridging region (where the two skins are bonded together) will experience opening stresses due to the initial stiffness of the core, with large stress concentrations at the edges of the core cells. Fillets of resin (made from Hexcel M21 film) will therefore be used to prevent delamination (see Figure 1a).

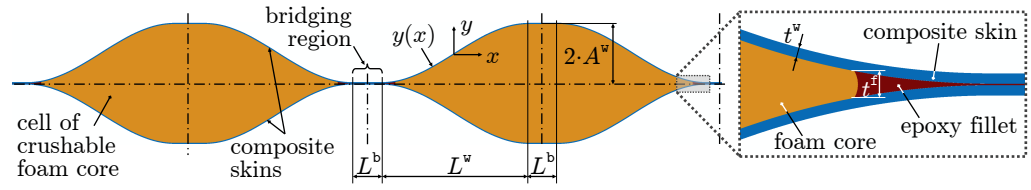

(a) Original configuration.

(b) Deformed configuration.

Figure 1: Wavy–ply sandwich concept.

2. Modelling and design

2.1. Analytical modelling and wave geometry design

The strength and maximum extension of the wavy–ply sandwich structure under remote tension can be estimated through the analysis of the wavy skins (of thickness t^{w}) under bending coupled with tension, neglecting the presence of the (by then failed) foam. Consider the sinusoidal curve $y(x)$ represented in Figure 1a, defined as:

$$y(x) = \alpha{\cdot}L^{w}{\cdot}\sin(\pi{\cdot}x/L^{w}) \,, \qquad \text{where} \qquad \alpha = A^{w}/L^{w} \,. \tag{1}$$

Let X_{∞} and e_{∞} be respectively the remote strength (normalised by the thickness of the skins, $2{\cdot}t^{w}$) and failure strain of the wavy–ply structure. Failure will ideally occur when the wavy skins are completely flattened (i.e. the foam core is completely crushed and the deflection is $v(x) = -y(x)$), under the combination of remote tensile stresses (X_{∞}) and maximum bending stresses (σ_{B}^{max}). If E_{T1}^{p} and X_{T1}^{p} are respectively the stiffness and strength of the composite plies in longitudinal tension, then X_{∞} must verify:

$$X_{T1}^{p} = X_{\infty} + \sigma_{B}^{max} \,, \qquad \text{with} \quad \sigma_{B}^{max} = \frac{t^{w}}{2}{\cdot}\left.\frac{\mathrm{d}^{2}y}{\mathrm{d}\,x^{2}}\right|^{max}{\cdot}E_{T1}^{p} \,. \tag{2a}$$

The overall strain will have contributions from the extension and the unfolding of the skins. If s^{w} is the half–wave arc–length, then e_{∞} will be:

$$e_{\infty} = \frac{X_{\infty}}{E_{T1}^{p}} + \frac{s^{w} - L^{w}}{L^{w} + L^{b}} \,, \qquad \text{with} \quad s^{w} = 2{\cdot}\int_{x=0}^{L^{w}/2} \sqrt{1 + \left(\frac{\mathrm{d}\,y}{\mathrm{d}\,x}\right)^{2}}\,\mathrm{d}x \,. \tag{2b}$$

Replacing the derivatives of Equation 1 into Equation 2 yields:

$$X_{\infty} = X_{T1}^{p} - \frac{t^{w}}{L^{w}}{\cdot}\frac{\alpha{\cdot}\pi^{2}}{2}{\cdot}E_{T1}^{p} \,, \tag{3a}$$

$$e_{\infty} = \frac{X_{T1}^{p}}{E_{T1}^{p}} - \frac{t^{w}}{L^{w}}{\cdot}\frac{\alpha{\cdot}\pi^{2}}{2} + \frac{L^{w}}{L^{w} + L^{b}}{\cdot}\left[\frac{2{\cdot}\sqrt{1 + \alpha^{2}{\cdot}\pi^{2}}}{\pi}{\cdot}\mathcal{E}\left(\frac{\alpha{\cdot}\pi}{\sqrt{1 + \alpha^{2}{\cdot}\pi^{2}}}\right) - 1\right] \,, \tag{3b}$$

where $\mathcal{E}(k) = \int_{0}^{\pi/2} \sqrt{1 - k^{2}{\cdot}\sin^{2}(\theta)}\,\mathrm{d}\theta$ is the complete elliptic integral of second kind.

Figure 2 presents the remote strength and failure strain of different wavy–ply sandwich configurations, predicted by Equation 3. The wave profile highlighted in Figure 2a and described in Table 1 was selected, as it provides a reasonable balance between strength and ductility.

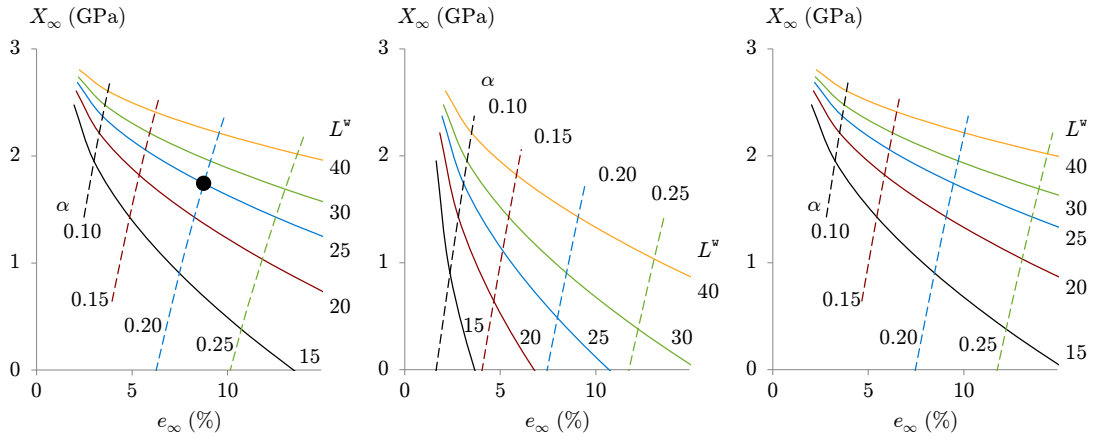

(a) $L^b = 5.0$ mm, $t^w = 1 \cdot t^p$. (b) $L^b = 5.0$ mm, $t^w = 2 \cdot t^p$. (c) $L^b = 2.5$ mm, $t^w = 1 \cdot t^p$.

Figure 2: Results from the analytical modelling for designing the wavy profile ($t^p = 0.193$ mm). The selected configuration (see Table 1) is shown as • in Figure 2a.

Table 1: Design parameters for the wavy–ply sandwich concept.

From analytical model (Section 2.1)					From FE simulations (Section 2.2)	
t^w (mm)	L^w (mm)	α (−)	A^w (mm)	L^b (mm)	t^f (mm)	Rohacell foam
0.193	25	0.20	5.0	5.0	0.5	RIMA-51

2.2. Finite element simulations and detailed design

The tensile response of the wavy–ply sandwich structure with nominal configuration (described in Table 1) was simulated using the FE package Abaqus; geometry and boundary conditions are represented in Figure 3, and material properties were obtained from datasheets and the literature [1–5]. Figures 4 and 5 show the results of the FE simulation for the optimised wavy–ply sandwich structure. The following sequence of events is predicted:

1. *Linear response* before the symbol □ in Figure 4a;
2. *Onset of plasticity in the foam core*, highlighted as □ in Figure 4a. Plastic deformation propagates across the height of the foam cell (see Figure 5a and 5b), and strains localise in bands due to the stress plateau in the response of the foam;
3. *Degradation of the skin–core interface* (between symbols ■ and ▲ in Figure 4a), as shown in Figures 5a and 5b. The skin–core interface does not debond completely, and begins closing after the point ▲ in Figure 4a;
4. *Strain hardening of the foam core* under compression (after the symbol ◇ in Figure 4a), developing a smooth crushing strain field (see Figures 5c and 5d);
5. *Extension of the CFRP skin* with progressive increase of the remote load (after the symbol ◇ in Figure 4a). The strain hardening in the global stress–strain curve is due to strain–hardening of the foam and re-alignment of the fibres along the loading direction;
6. *Catastrophic failure* of the CFRP skins (highlighted as × in Figure 4a). Tensile failure (due to remote and bending stresses) is triggered at the outer surface of the skin near the the epoxy fillet (see Figure 5d), and propagates unstably across the skin thickness.

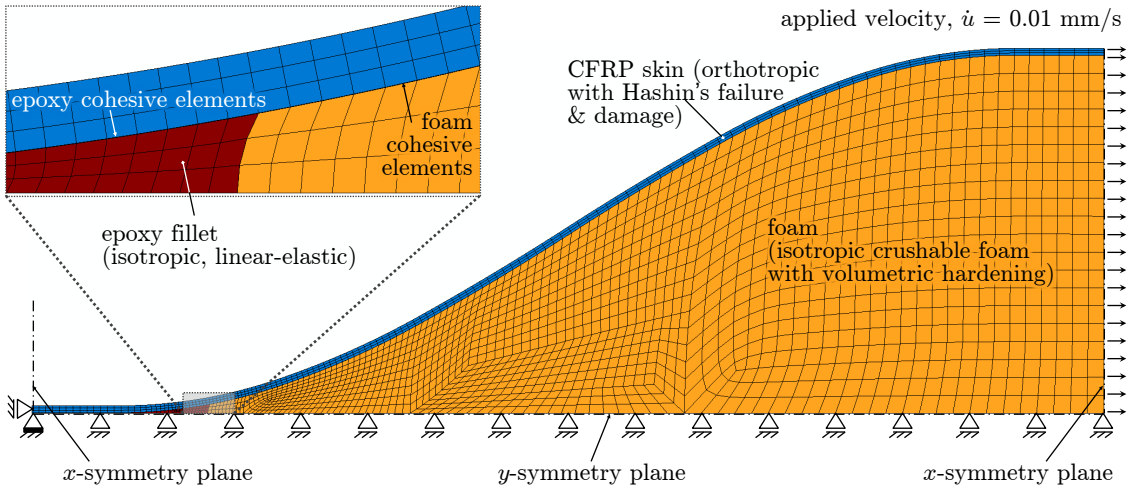

Figure 3: Overview of the FE model (with optimised geometry, as described in Table 1).

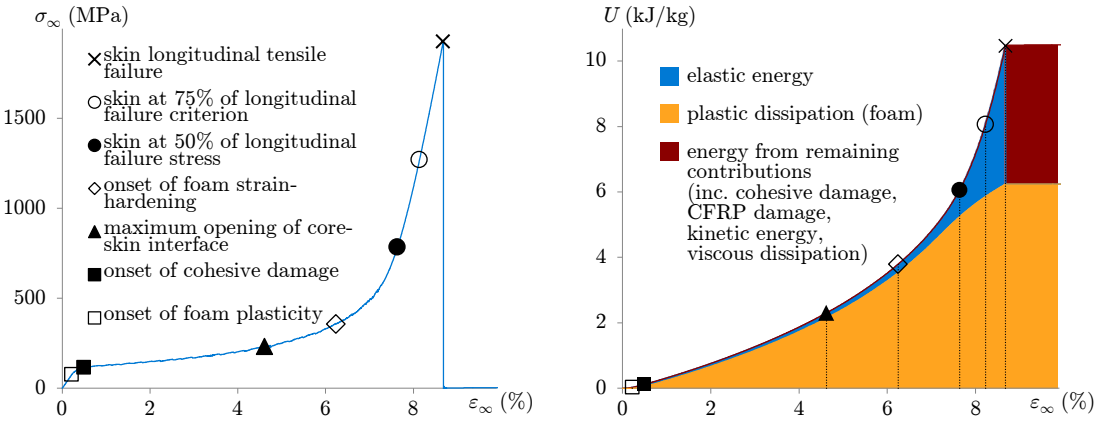

(a) Overall stress–strain curve.

(b) Energy components.

Figure 4: Response predicted by FE for the nominal wavy–ply sandwich configuration.

The effect of varying the core material is presented in Figure 6a. Using a lighter foam (IG–31 [6]) did not affect the sequence of events previously described, but it reduced the support provided to the composite skins. Consequently, lower initial stiffness, yield stress and ultimate strength were predicted for the sandwich structure with lighter foam core. Increasing the density of the foam core (RIMA–71 [4] in Figure 6a) delayed the onset of core crushing, thus increasing the initial stiffness and yield stress of the sandwich structure. However, this aggravated the degradation of the skin–foam interface comparatively to the nominal configuration (see Figure 5b) and led to full delamination of the bridging region.

Figure 6b shows the influence of the thickness of the epoxy fillet on the response of the wavy–ply structure. A very thin fillet (t^{f} = 0.2 to 0.3 mm in Figure 6b) is unable to arrest degradation of the skin–core interface and delamination of the bridging region. It was predicted that this failure mode could be avoided by using fillets with $t^{\mathrm{f}} \geq 0.4$ mm; however, increasingly thicker fillets create larger bending stresses, thus reducing slightly the ultimate strength of the sandwich structure (see curves for t^{f} = 0.4 to 0.6 mm in Figure 6b).

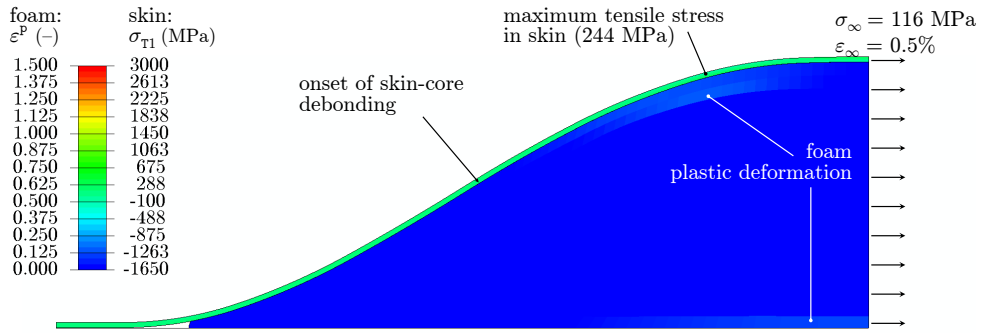

(a) At the onset of cohesive damage (■ in Figure 4a).

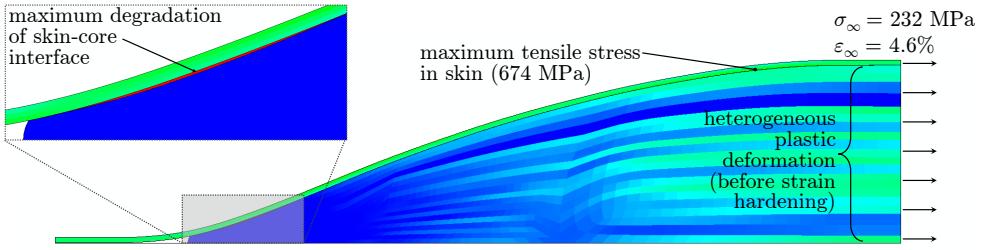

(b) At maximum opening of the core-skin interface (▲ in Figure 4a).

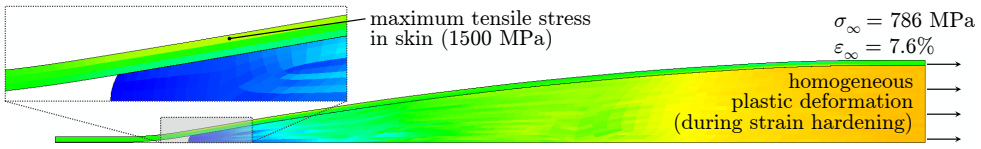

(c) At 25% of the skin longitudinal failure criterion (● in Figure 4a).

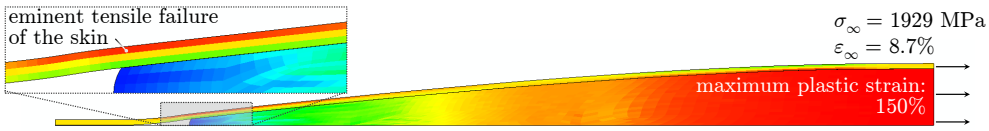

(d) Immediately before longitudinal tensile failure of the skin (× in Figure 4a).

Figure 5: Deformed shape, equivalent plastic strains in the foam core, and longitudinal stresses in the CFRP skin, as predicted by the FE analysis for the nominal configuration.

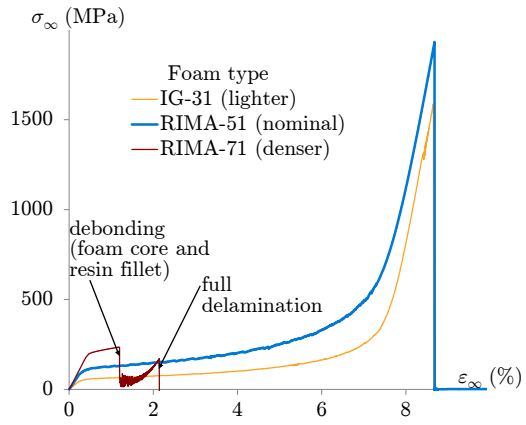

(a) Effect of foam type.

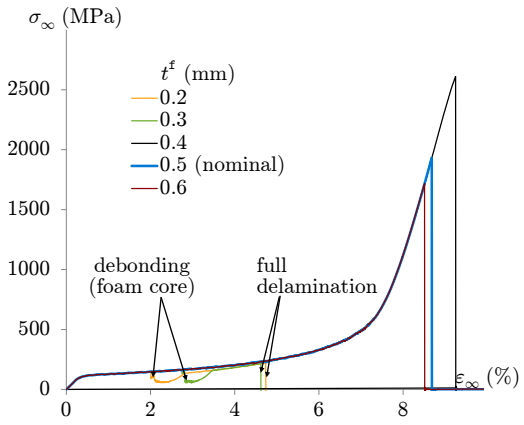

(b) Effect of fillet thickness.

Figure 6: Parametric study on the predicted response of wavy–ply sandwich structures.

3. Experimental procedure

The wavy–ply sandwich concept was demonstrated by manufacturing and testing two sets (A and B) of specimens (see Figures 7 and 8a). The sets differed in the epoxy fillet: the edges of the foam cells in Set B were lightly sanded (thus increasing slightly t^{f}), and the epoxy fillet was manually moulded from resin film in a round shape before curing; these changes were aimed at reducing void formation in the fillet region, which had been observed in Set A (see Figure 8b).

Specimens (as in Figure 8a) were loaded under tension at 1 mm/min. Remote stresses were calculated as $\sigma_\infty = P/(w_{\mathrm{spec}} \cdot t_{\mathrm{nom}})$, where P is the overall load, w_{spec} is the measured specimen width, and $t_{\mathrm{nom}} = 0.386$ mm is the nominal thickness of the bridging region. Strains (see ε_1, ε_2, and ε_3 in Figure 8a) were measured using an optical extensometer system.

4. Results from experimental characterisation

Remote stress–strain curves for all specimens tested are shown in Figure 9 (remote strains (ε_∞) correspond to the average strain of at least two wavelengths, see Figure 8a). Set A was largely unsuccessful (Figure 9a), with six specimens failing by delamination (Figure 10a) triggered by voids at the bridging region (Figure 8b). Only one specimen (coincidently without any visible voids) of Set A exhibited a ductile response (illustrated in Figure 10b).

Avoiding void formation in Set B resulted in six (out of eight) successful tests (Figure 9b). The statistics for the initial stiffness (E_0), ultimate strength (X_∞), failure strain (e_∞) and specific work of fracture (U) of valid specimens of Set B are shown in Table 2.

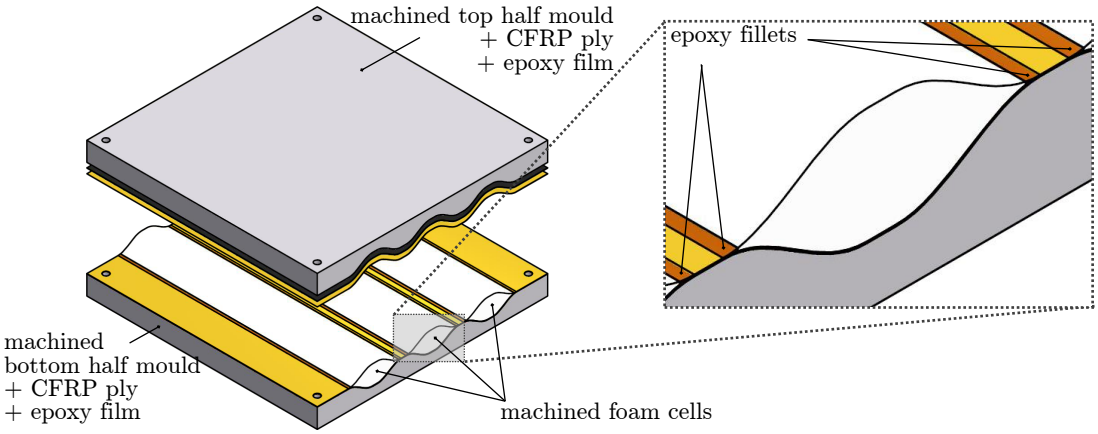

Figure 7: Schematic lay-up of a wavy–ply sandwich panel.

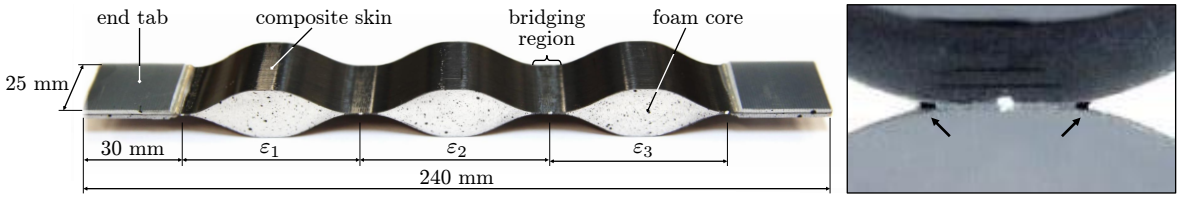

(a) Dimensions and definition of strain measurements ($\varepsilon_i \approx 60$ mm). (b) Voids in bridging region.

Figure 8: Wavy–ply sandwich specimen.

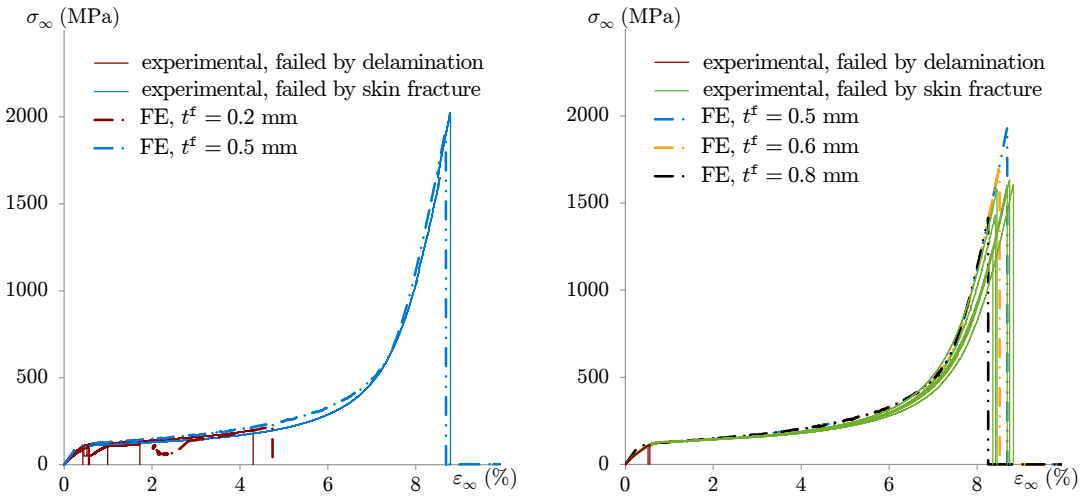

(a) Set A. (b) Set B.

Figure 9: Stress–strain curves of all specimens tested, and comparison with FE predictions.

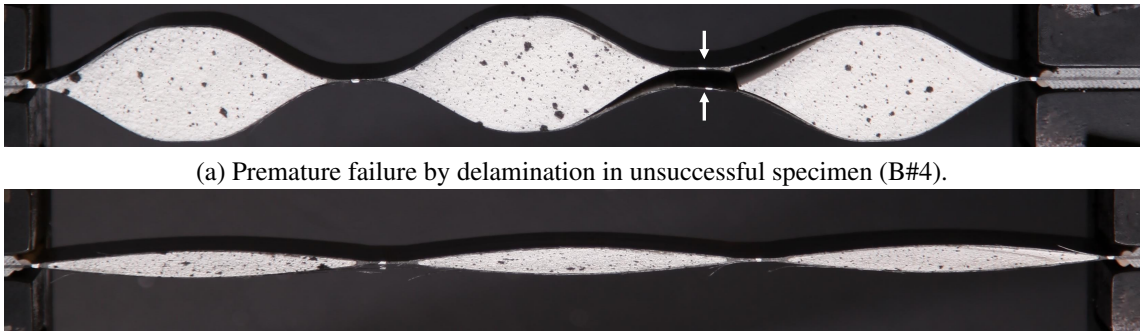

(a) Premature failure by delamination in unsuccessful specimen (B#4).

(b) Large deformations in successful specimen (B#6), immediately before explosive skin failure.

Figure 10: Different failure modes observed in wavy–ply sandwich specimens.

Table 2: Mechanical properties measured for wavy–ply composites (six valid tests of Set B).

	E_0	X_∞	e_∞	$U^{(\star)}$
Average	28.4 GPa	1570 MPa	8.62%	9.35 kJ/kg
Coefficient of Variation	2.9%	5.0%	2.1%	9.6%
Monolithic CFRP specimen	165 GPa	3000 MPa	1.82%	–

$^{(\star)}$ Estimated from a calculated areal weight for the wavy–ply sandwich of 1198 g/m^2.

5. Discussion

The agreement between experimental results and blind FE predictions shown in Figure 9 is remarkable, especially considering the several sources of geometric and material non-linearity in the structure, as well as the different failure modes observed.

Table 2 shows that the wavy–ply sandwich concept can increase the failure strain of CFRP plies by nearly one order of magnitude and dissipate a considerable amount of energy. This compensates for the decrease in stiffness and strength and for the increase in areal weight.

The symmetric wavy–ply concept developed in this paper presents the following advantages:

- It generates a smooth stress–strain response, where the load increases continuously with deformation (see successful specimens in Figure 9b) and the energy is dissipated stably. This is a main advantage over asymmetric wavy–ply sandwich structures [7];
- A great component of energy dissipated (6.2 kJ/kg, as shown in Figure 4b) is absorbed through crushing of the core, which retains significant permanent deformation;
- Failure strains above 8.6% were measured in specimens with brittle CFRP skins. Using high performance ductile fibres (e.g. ultra-high-molecular-weight polyethylene fibres) as skin material can potentially double the measured failure strain.

6. Conclusions

This paper presented a new wavy–ply sandwich structure developed to achieve large deformations and energy absorption under tensile loading. The wave profile was designed using an analytical formulation combining the effect of remote tension and bending (i.e. unfolding) of the skins. Finite element analyses supported the selection of the core material and resin fillet geometry, in order to avoid premature failure by delamination in the bridging region.

Results from experimental tensile tests showed an excellent correlation with modelling predictions. This work demonstrated that wavy–ply sandwich structures with CFRP skins can withstand remote deformations of 8.6% and dissipate 9.4 kJ/kg under tensile load. Future work will focus on improving these figures further, and exploring the potential of the wavy–ply sandwich concept for blast–protection structures and protective layers in pressurised vessels.

Acknowledgements

This work was funded under the EPSRC Programme Grant EP/I02946X/1 on High Performance Ductile Composite Technology, in collaboration with the University of Bristol. The authors thankfully acknowledge the contribution from N. Hallstein and H. Yasin from Evonik Industries AG, for providing the foam material and for their helpful advice.

References

[1] Z. Jehangir. Experimental investigation of the translaminar ply fracture toughness of advanced composites. MEng Project Report, Imperial College London, UK, 2011.

[2] M. Ilyas et al. Dynamic delamination of aeronautic structural composites by using cohesive finite elements. In *17th International Conference on Composite Materials*, Edinburgh, 27–31 July 2009.

[3] M.J. Laffan et al. Translaminar fracture toughness testing of composites: A review. *Polymer Testing*, 31(3):481–489, 2012.

[4] S. Arezoo et al. The mechanical response of Rohacell foams at different length scales. *Journal of Materials Science*, 46(21):6863–6870, 2011.

[5] E.Saenz et al. Mode I fracture toughness of PMI sandwich core materials. In *8th International Conference on Sandwich Structures*, Porto, 6–8 July 2008.

[6] R. Juntikka and S. Hallstrom. Weight–balanced drop test method for characterization of dynamic propertiesof cellular materials. *International Journal of Impact Engineering*, 30(5):541–554, 2004.

[7] C. Winkelmann et al. Design and development of hybrid composite bistable structures for energy absorption under quasi-static tensile loading. *Composite Structures*, 93(1):171–178, 2010.